Application of Fluorescence Emission for Characterization of Albendazole and Ricobendazole Micellar Systems: Elucidation of the Molecular Mechanism of Drug Solubilization Process

Josefina Priotti, Darío Leonardi, Guillermo Pico & María C. Lamas

AAPS PharmSciTech
An Official Journal of the American Association of Pharmaceutical Scientists

e-ISSN 1530-9932

AAPS PharmSciTech
DOI 10.1208/s12249-017-0927-6

Springer

AAPS PharmSciTech (© 2017)
DOI: 10.1208/s12249-017-0927-6

Research Article

Application of Fluorescence Emission for Characterization of Albendazole and Ricobendazole Micellar Systems: Elucidation of the Molecular Mechanism of Drug Solubilization Process

Josefina Priotti,[1] Darío Leonardi,[1,2] Guillermo Pico,[3,4] and María C. Lamas[1,2,5]

Received 3 October 2017; accepted 25 November 2017

Abstract. Albendazole (ABZ) and ricobendazole (RBZ) are referred to as class II compounds in the Biopharmaceutical Classification System. These drugs exhibit poor solubility, which profoundly affects their oral bioavailability. Micellar systems are excellent pharmaceutical tools to enhance solubilization and absorption of poorly soluble compounds. Polysorbate 80 (P80), poloxamer 407 (P407), sodium cholate (Na-C), and sodium deoxycholate (Na-DC) have been selected as surfactants to study the solubilization process of these drugs. Fluorescence emission was applied in order to obtain surfactant/fluorophore (S/F) ratio, critical micellar concentration, protection efficiency of micelles, and thermodynamic parameters. Systems were characterized by their size and zeta potential. A blue shift from 350 to 345 nm was observed when ABZ was included in P80, Na-DC, and Na-C micelles, while RBZ showed a slight change in the fluorescence band. P80 showed a significant solubilization capacity: S/F values were 688 for ABZ at pH 4 and 656 for RBZ at pH 6. Additionally, P80 micellar systems presented the smallest size (10 nm) and their size was not affected by pH change. S/F ratio for bile salts was tenfold higher than for the other surfactants. Quenching plots were linear and their constant values (2.17/M for ABZ and 2.29/M for RBZ) decreased with the addition of the surfactants, indicating a protective effect of the micelles. Na-DC showed better protective efficacy for ABZ and RBZ than the other surfactants (constant values 0.54 and 1.57/M, respectively), showing the drug inclusion into the micelles. Entropic parameters were negative in agreement with micelle formation.

KEY WORDS: micellar systems; albendazole; ricobendazole; solubilization; polysorbate 80; poloxamer 407; bile salts; fluorescence.

INTRODUCTION

Serious global health problems are caused by helminthic infections, which are among the most common diseases worldwide. More than 1.5 billion people are infected, and approximately 300 million people suffer from severe morbidity which leads to more than 150,000 deaths annually (1,2). The greatest numbers of helminthic infections occur in sub-Saharan Africa, East Asia, China, India, and South America (3). Albendazole (ABZ) and ricobendazole (RBZ) are wide-spectrum anthelmintic drugs often used against gastrointestinal parasites. Their mechanism of action is related to microtubule inhibition and glucose uptake blockage in the larval and adult stages of susceptible parasites (4). Chemically, both compounds are benzimidazole drugs: ABZ is methyl 5-(propylthio)-2-benzimidazole-carbamate and RBZ (or ABZ sulfoxide) is the active metabolite of ABZ (Fig. 1a) (5,6). ABZ is practically insoluble in water (1 μg/mL); slightly soluble in acetone, chloroform, and ethanol; and soluble in acetic acid (7–9). RBZ also has low aqueous solubility (62 μg/mL), very poor solubility in oils (< 0.25 mg/mL), ethanol (1.2 mg/mL), propylene glycol (2.6 mg/mL), and slightly higher solubility in dipolar solvents such as DMSO (16.5 mg/mL) (10,11). U-shaped pH-solubility profile in aqueous solutions indicates that RBZ is an ampholyte. It has been reported that the combination of low pH and surfactant/co-solvent mixtures improve its solubility (10).

Both ABZ and RBZ are aromatic compounds which have the property of fluorescence emission as a result of the benzimidazole group present in their molecules (12–14).

[1] IQUIR-CONICET, Suipacha 570, S2002LRK, Rosario, Argentina.
[2] Departamento de Farmacia, Facultad de Ciencias Bioquímicas y Farmacéuticas, Universidad Nacional de Rosario, Suipacha 570, S2002LRK, Rosario, Argentina.
[3] IPROBYQ- CONICET, Suipacha 570, S2002LRK, Rosario, Argentina.
[4] Departamento de Química-Física, Facultad de Ciencias Bioquímicas y Farmacéuticas, Universidad Nacional de Rosario, Suipacha 570, S2002LRK, Rosario, Argentina.
[5] To whom correspondence should be addressed. (e–mail: mlamas@fbioyf.unr.edu.ar)

Published online: 07 December 2017

Several fluorescence probes have been used to measure protein-membrane interactions (15). Moreover, probes can be used to follow a solubilization equilibrium and to obtain information about its molecular mechanism (16,17).

In the last decades, polymeric surfactants have emerged as a class of materials with a wide range of pharmaceutical applications. Polymeric surfactants form nanoscopic core-shell structures above the critical micellar concentration (cmc), which have the ability to solubilize poorly soluble drugs (18,19). The hydrophobic cores can be employed as delivery systems for hydrophobic drugs while the hydrophilic part can be used as an interface between the bulk aqueous phase and the hydrophobic domain. Several hundreds of ionic surfactants have been used to solubilize poorly soluble substances. Some of them are more efficient but toxic, which limits their use. The ideal surfactant should be compatible with the cellular metabolism and also easily eliminated by the organism (20).

Synthetic surfactants, such as the polysorbate and poloxamer families, have been shown to be non-toxic and biocompatible. Polysorbates (also known as Tweens®) are a class of non-ionic surfactants which are esters of fatty acids and PEGylated sorbitols. Due to their significant stability and non-toxicity, they have wide applications in the pharmaceutical, cosmetic, and food industries (21). Polysorbate 80 (P80) is a derivative molecule from polyethoxylated sorbitan and oleic acid, the hydrophilic groups being polyethers, which are polymers of ethylene oxide (Fig. 1b). P80 presents the remarkable property of being extremely biodegradable under aerobic and anaerobic conditions even by not specialized soil bacteria (22).

Poloxamers (also known as Pluronics®) are triblock copolymers consisting of a central hydrophobic block of polypropylene glycol flanked by two hydrophilic blocks of polyethylene glycol (23,24). Regarding the poloxamer 407 (P407) chemical structure, the approximate length of the two polyethylene glycol blocks is 100 repeated units while the approximate length of the propylene glycol block is 65 repeated units, as shown in Fig. 1c (25).

Another interesting possibility to develop micellar systems is the use of natural surfactants such as the family of bile salts. Bile salts are amphipathic molecules with a hydrophilic side containing hydroxyl groups (α-side) and a hydrophobic side with methyl groups (β-side) (26,27). This makes them very different from the traditional surfactants employed in pharmaceutical formulations, which are often composed of a polar head group and a long non-polar tail. Sodium cholate (Na-C) and sodium deoxycholate (Na-DC) are bile salts that differ only in a hydroxyl group (Fig. 1d) (28). Several studies have been focused on the solubilizing effect of bile salts on

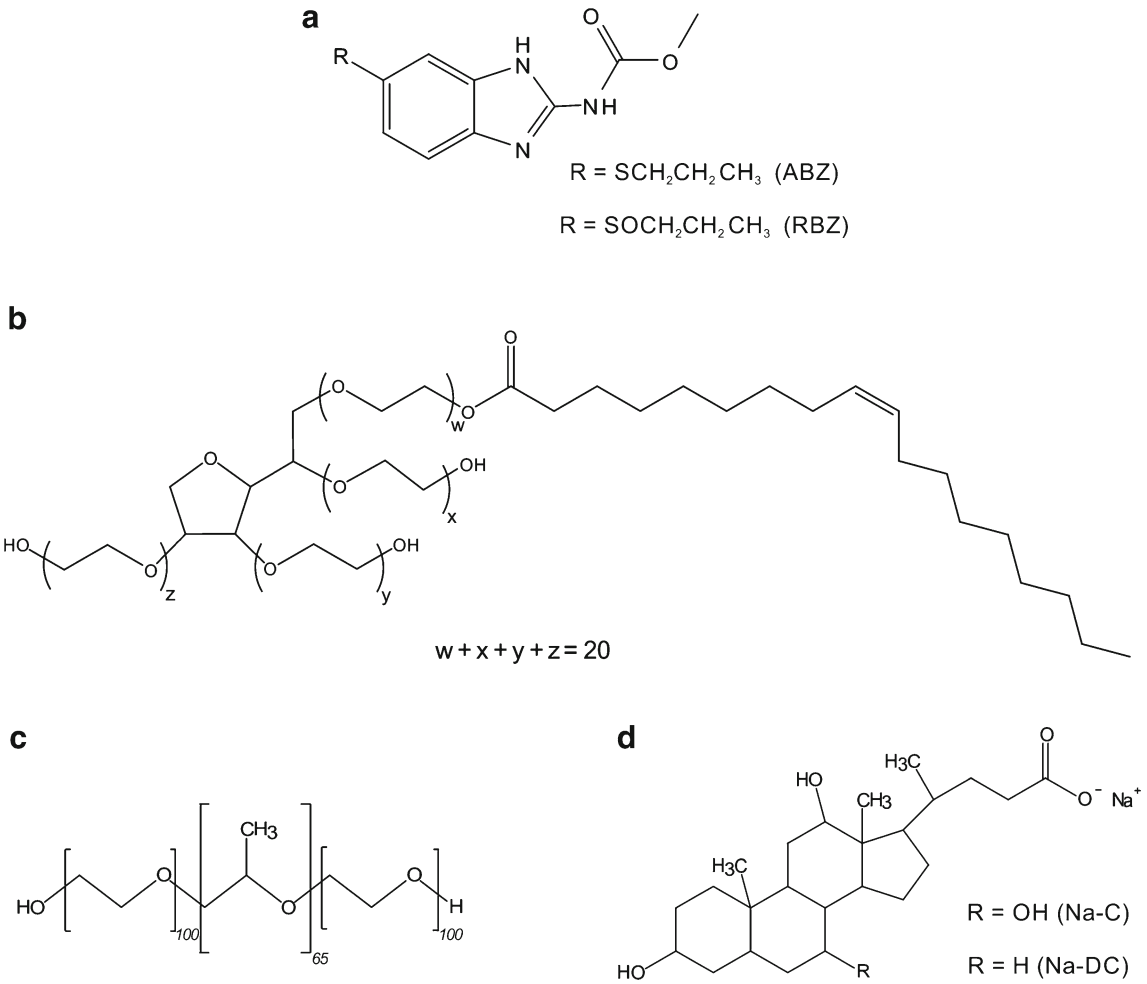

Fig. 1. Molecular structures of **a** ABZ and RBZ, **b** P80, **c** P407, and **d** Na-C and Na-DC

poorly water-soluble drugs in different formulations (27,29). Thus, the aim of the present work was to study the capacity of two physiological surfactants, Na-C and Na-DC, and two synthetic flexible chain polymer surfactants, P407 and P80, to solubilize the poorly soluble anti-parasitic agents: ABZ and RBZ.

MATERIALS AND METHODS

Materials

ABZ (lot 035K1421), RBZ (lot BCBP1728V), P80, Na-C, and Na-DC were purchased from Sigma-Aldrich Chemie GmbH (Steinheim, Germany), all more than 98% pure. P407 (Pluronic® F127, average molecular weight 12.6 kDa) was purchased from BASF (NJ, USA). Dimethyl sulfoxide anhydrous (DMSO) ≥ 99.9% was obtained from Sigma-Aldrich Chemie GmbH (Steinheim, Germany). All other chemicals were of analytical grade.

Methods

Solutions

ABZ and RBZ solutions were prepared in DMSO (1 and 3 mg/mL, respectively). Surfactant solutions (5% *w/v*) were prepared by dissolving in citric acid-sodium phosphate dibasic buffer (pH 4.0, 6.0, and 7.0). P407 and P80 were dissolved at pH 4.0 and 6.0 while bile salts were prepared at pH 7.0 due to their pKa (Na-C, 6.4, and Na-DC, 6.6).

Mathematical Model for the Study of the Surfactant—ABZ and RBZ Inclusion Equilibrium. Fluorescent probes have been widely applied to study micelle formation in surfactants. The method is based on the polarity change in the dielectric constant of the microenvironment where the probe is included in the micelle (30). The micelle formation process may be written in a simplified form according to the method reported by Sepúlveda and Pérez-Cotapos (31) by the following equilibrium:

$$X + D_m \leftrightarrow X\text{-}D_m \tag{1}$$

where

X The optical probe
D_m The surfactant under the micelle form

K_x is the equilibrium constant of micelle formation in the presence of the optical probe, defined as follows:

$$K_x = \frac{[X\text{-}D_m]}{[X][D_m]} \tag{2}$$

[X - D_m] is the total molar concentration of the optical probe incorporated to the micelle, *[X]* the free concentration of the optical probe in water and *[D_m]* the concentration of the surfactant below the cmc. Assuming that the fluorescence emissions of the optical probe are F_o in the absence of surfactant, F_i in the presence of i concentration of surfactant and F_m when all the optical probe is included in the micelle, the fraction of optical probe (f) in the micelle can be calculated as

$$f = \frac{F_i - F_m}{F_0 - F_m} \tag{3}$$

It is easy to demonstrate the following relationship between K_x and f:

$$\frac{f}{1-f} = K_x([D_t] - [X_t]) \tag{4}$$

where *[D_t]* and *[X_t]* are the total concentrations of surfactant and optical probe in the medium, respectively.

A plot of $f/(1-f)$ *versus* $([D_t] - [X_t])$ yields a strength line with a slope of K_x (31).

The thermodynamic function values (standard Gibbs energy (ΔG), enthalpic (ΔH), and entropic changes (ΔS)) were estimated by applying thermodynamic Eqs. 5, 6, and 7 as follows:

$$\Delta G = -RT\ln(K_x) \tag{5}$$

$$\ln\left(\frac{K_1}{K_2}\right) = \frac{\Delta H}{R}\left(\frac{1}{T_1} - \frac{1}{T_2}\right) \tag{6}$$

$$\Delta G = \Delta H - T\Delta S \tag{7}$$

where K_1 and K_2 are the equilibrium constants at temperature T_1 and T_2, respectively, R is the universal gas constant (8.3×10^3 kJ/mol K), and T is the absolute temperature (30,32,33).

Fluorometric Titration of ABZ and RBZ by Addition of the Surfactants. ABZ and RBZ stock solutions (5 μL) were added to citric acid-sodium phosphate dibasic buffer to obtain a final solute concentration of 6.3×10^{-3} and 17×10^{-3} mM, respectively. The final concentration of DMSO was lower than 0.1% (*v/v*). Thus, the effect on the fluorescence emission in aqueous medium can be considered negligible. Aliquots of 5 to 30 μL of surfactant solutions were added to the buffer containing the fluorophore. Then, the fluorescence emission spectrum was obtained between 310 and 430 nm (exciting at 294 nm) for ABZ, and between 300 and 400 nm (exciting at 290 nm) for RBZ. Spectrofluorometric measurements were performed on an Aminco Bowman S2 spectrofluorometer (AB2, Rochester, NY) using a thermostatized 1-cm path length cell.

Localization of ABZ and RBZ Incorporated in the Surfactant Micelle. The solvent accessibility to the optical probe incorporated in the micelle can be easily determined by the fluorescence quenching technique. If the fluorescent probe is situated in a micelle area where the solvent is accessible to the quencher (Q), which is the substance able to decrease the fluorescence emission, Q will have access to the

fluorescent probe and will induce a decrease in its fluorescence. If Q cannot have access to the optical probe, the fluorescence emission of the probe will not be modified. The Stern-Volmer equation relates the intensity of the fluorescence to the Q concentration in a quantitative form through the Eq. 8:

$$\frac{I_0}{I_i} = 1 + K[\mathrm{Q}] \tag{8}$$

where I_o and I_i are the fluorescence intensities of the optical probe included in the micelle in the absence and presence of i concentration of Q; K is the quenching constant, which is directly related to the capacity of Q to have access to the optical probe. In micelles where the optical probe is not accessible to the solvent, K values are low (protective effect of the micelle) while K value is maximum in the absence of surfactant (free optical probe) (34). This method enables us to determine the position of the optical probe molecule in the micelle. The determination of K was carried out by measuring the fluorescence emission of the probe incorporated in the micelle after the addition of different concentrations of acrylamide, which was used as Q. The experiment was performed using the minimum concentration surfactant solutions to solubilize the drugs. Then, samples were titrated with acrylamide solution (12 M). ABZ or RBZ fluorescence emission intensity was measured at 350 and 324 nm, exciting at 294 and 290 nm, respectively. The experiments were performed in triplicate, and the results were analyzed using the Stern-Volmer equation.

Zeta Potential and Size of the Surfactant Micelles with ABZ and RBZ Included. A Zetasizer Nano ZS90 (Malvern Instruments, Worcestershire, UK) using dynamic light scattering (DLS) was employed to measure the micelle size and zeta potential (Zp). Surfactant solutions with ABZ or RBZ were prepared in citric acid-sodium phosphate dibasic buffer, varying the pH value from 4.0 and 7.0. Micelle sizes (hydrodynamic diameter) were measured by taking into account the first order result from a DLS experiment as an intensity distribution of the particle size. The intensity distribution was weighed according to the scattering intensity of each particle fraction or family. All analyses were carried out three times and sample readings were done in triplicate within an angle of 90 at 25°C.

RESULTS

Effect of the Surfactant on the ABZ and RBZ Fluorescence Emission Spectrum

No fluorescence change was observed in the course of time, after the addition of surfactant aliquots which suggests that the inclusion of ABZ or RBZ in the surfactant micelle is a very fast process. ABZ aqueous solution showed a well-defined emission peak at 350 nm (exciting at 294 nm). The presence of P407 did not induce any significant shift in the position of the ABZ fluorescence band. However, a little enhancement in the fluorescence emission was observed, suggesting an increase in the population of the exited state of ABZ (Fig. 2). A significant blue shift of the band position with an enhancement of the fluorescence emission was induced by Na-C, Na-DC, and P80 (Table I). Therefore, ABZ can be used as an optical probe to measure the polarity of the environment where its molecule is included.

Table I shows that the new emission peak position was displaced around 6 nm as is the case of Na-DC. On the other hand, the assayed surfactants did not produce any effect on the RBZ fluorescence spectrum. The micro-dielectric constants (Ds) of the environments where ABZ or RBZ are situated in the micelle of the surfactants were calculated from their fluorescence spectra in ethanol-buffer mixtures and are shown in Table I.

Solubilization of ABZ and RBZ by P80, P407, and Bile Salt Solutions

ABZ solutions at 6.3×10^{-3} mM were titrated with increased concentrations of P80, P407, and bile salts. Figure 3 shows ABZ titration with P80 and P407. Titration curves were expressed as the change in fluorescence intensity (ΔF) *versus* surfactant concentration.

The curves had a hyperbolic shape for P80, while Na-C, Na-DC, and P407 showed a sigmoidal behavior, in agreement with previous reports (16). In all cases, the fit curves reached a plateau, suggesting the presence of a saturation process in micelle formation.

The cmc of these surfactants in the presence of ABZ was calculated from the non-linear fitting of the ΔF *versus* the total concentration of the surfactant. The cmc was estimated as the surfactant concentration where 50% of fluorescence change is observed. The values of cmc for the surfactants assayed are shown in Table I. The values observed for the surfactants in the presence of the anthelmintic compounds are higher than those in their absence (cmc values of the surfactants previously reported) (16,35,36).

The surfactant/fluorophore stoichiometry (S/F) ratio for the solubilization capacity of the surfactants was determined from the fluorometric titrations (Table I). S/F gives the surfactant the necessary mass to solubilize the mass unity of fluorophore. As it can be seen from Table I, P80 showed the best

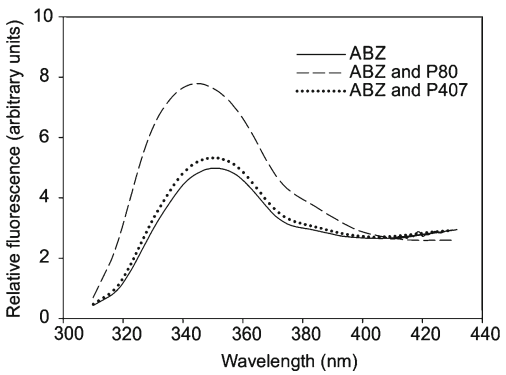

Fig. 2. Fluorescence emission spectrum of ABZ (6.3×10^{-3} mM) in the absence and presence of non-ionic surfactants, P407 (0.0802 mM) and P80 (0.747 mM) in citric acid-sodium phosphate dibasic buffer (pH 4.0), 20 °C

Table I. Physicochemical Parameters that Show the Solubilization Capacity of the Surfactants, Surfactant/fluorophore (S/F) Ratio and Critical Micellar Concentration (cmc) to ABZ (3.77 μM) and RBZ (3.55 μM), Stern-Volmer Constant (*K*) Values, Maximum Emission Wavelength (λ_{max}), and Microdielectric Constant (D)

	Surfactant	pH	S/F (*w*/*w*)	cmc (mM)	*K* (/M)	λ_{max} (nm)	D
ABZ	None	–	–	–	2.17 ± 0.05	350	79.7
	P80	4.0	688 ± 4	0.343 ± 0.002	0.79 ± 0.05	345	56.1
	P80	6.0	1527 ± 4	0.679 ± 0.002	0.59 ± 0.02	344	36.3
	P407	4.0	860 ± 3	0.071 ± 0.002	1.28 ± 0.03	351	78.1
	P407	6.0	1410 ± 3	0.116 ± 0.003	0.88 ± 0.03	349	76.5
	Na-C	7.0	7590 ± 20	17.63 ± 0.04	0.93 ± 0.04	343	47.0
	Na-DC	7.0	4470 ± 122	10.8 ± 0.3	0.54 ± 0.03	344	51.7
RBZ	None	–	–	–	2.29 ± 0.03	325	89.0
	P80	4.0	688 ± 4	0.343 ± 0.002	2.07 ± 0.04	325	87.5
	P80	6.0	656 ± 1	0.259 ± 0.002	2.23 ± 0.07	325	88.8
	Na-C	7.0	4530 ± 10	5.99 ± 0.01	2.11 ± 0.06	324	78.7
	Na-DC	7.0	7110 ± 20	8.71 ± 0.02	1.57 ± 0.02	324	78.7

solubilization capacity for ABZ at pH 4.0, and good solubilization capacity for RBZ at pH 6.0, with respect to the other surfactants assayed. The physiological surfactants (Na-C and Na-DC) showed concentrations tenfold higher than those of the other two surfactants to solubilize the same amount of fluorophore. This finding may be due to the different micelle structure of the synthetic surfactants compared to the bile salts. The latter have a planar spatial structure, which produces the formation of "sandwich" micelles, with a low capacity to introduce the hydrophobic solute in its interior, whereas P80 and P407 produce spherical micelles which facilitate the inclusion of the fluorophores (26,37).

K_x (the equilibrium constant for the micelle formation process) in the presence of ABZ was calculated using Eqs. 1–4. The results obtained for the different surfactants are shown in Table II. The micelle formation equilibrium was measured at two different temperatures (293 and 310 K) and the values of the thermodynamic function associated to the equilibrium were calculated by applying Eqs. 5–7 (Table II).

The enthalpy associated with the micelle formation in the presence of ABZ showed minor changes, while the entropic changes were negative, in agreement with the formation of an ordered structure (the micelle). However, the low enthalpy values suggest the loss of water structure around the hydrophilic zones or chains of the surfactants when the micelle is formed (30).

Quenching of the ABZ and RBZ Fluorescence Included in the Surfactant Micelle

Quenching experiments were employed to evaluate the protection efficiency that surfactant micelles produce to the incorporated ABZ or RBZ molecules. The fluorescence intensity in the absence and presence of surfactant decreased with the increase of acrylamide concentration.

Quenching plots were linear (Fig. 4), which suggests that the molecular mechanism is only collisional. *K* values, calculated from Eq. 8, decreased in the presence of all the surfactants assayed, in comparison with the value observed in the absence of surfactants (Table I), suggesting a partial protective effect of the surfactants from the attack of the acrylamide. These experiments were carried out at S/F ratio (above the cmc values) since, under this experimental condition, all the fluorophore molecules are included in the surfactant micelle and the free fraction of fluorophore is negligible. Therefore, the fluorescence quenching may be attributed only to the fluorophore in the micelle exposed to the solvent.

As low K values were observed, it can be assumed that a high protective effect on ABZ was produced by both P80 and Na-DC. These values indicated that ABZ was situated in a hydrophobic region of the micelle. On the other hand, considering the *K* values observed, the surfactants P80, P407 and Na-C had a low protective effect on RBZ while Na-DC showed a higher protective effect (Table I).

Micellar Size and Zp Analysis of the Surfactant Micelles in the Presence of ABZ and RBZ

Micelle formation implies the presence of an auto-ordered structure with electro-kinetics properties, such as electrical potential, which occurs not only when the surfactant has net electrical charge, like Na-DC and Na-C, but also with non-ionic surfactants. These surfactants in particular, have the capacity to absorb small ions from the medium in different ways, acquiring an electro-kinetic potential (38).

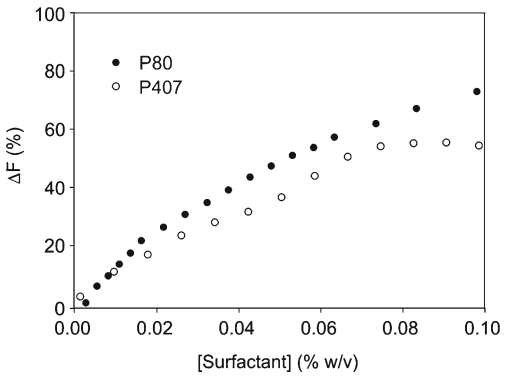

Fig. 3. Fluorometric titration curves of ABZ (6.3×10^{-3} mM) with increasing surfactant concentrations (P80 and P407) in citric acid-sodium phosphate dibasic buffer (pH 4.0), 20 °C

Table II. Thermodynamic Parameters of ABZ in the Presence of P80 and P407. Medium Citric Acid-sodium Phosphate Dibasic Buffer (pH 4.0), Temperature 293 K

Surfactant	K_x ($\times 10^5$/M)	$\Delta G°$ (kJ/mol)	$\Delta H°$ (J/mol)	$T\Delta S°$ (kJ/mol)
P80	2.67	−30.42	−79.15	−30.5
P407	2.79	−30.53	914	−29.6

Table III. Average Size, Polydispersity Index and Z Potential (Zp) Observed for the Surfactant Micelles in the Presence of ABZ and RBZ

	Surfactant	pH	Average size (nm)[a]	PI	Zp (mV)[a]
ABZ	P80	4	10.2 ± 0.3	0.277	−4.7 ± 0.9
	P80	6	10.1 ± 0.5	0.218	−4.4 ± 0.5
	P407	4	360 ± 159	0.967	−1.5 ± 0.2
	P407	6	459 ± 105	0.838	−0.0 ± 0.8
	Na-C	7	226 ± 20	0.764	−8.3 ± 0.6
	Na-DC	7	ND	ND	ND
RBZ	P80	4	9.8 ± 0.5	0.129	−6 ± 2
	P80	6	10.19 ± 0.08	0.144	−3.1 ± 0.6
	Na-C	7	101.7 ± 6.8	0.836	−16 ± 1
	Na-DC	7	49 ± 46	0.349	−42 ± 3

[a] The measurements were done in triplicate. Table shows mean ± standard deviations
PI polydispersity index (≤ 0.5 monodisperse; > 0.5 polydisperse), *ND* not determined

Table III shows average size, polydispersity index, and Zp observed for the surfactant micelles in the presence of the two anti-parasitic compounds. The effect of pH values was studied for P80 and P407 (according to the fluorometric titrations previously obtained).

The micellar size of P80 with ABZ and RBZ was not affected by pH variation, while P407-ABZ system showed an increase when pH varied from 4.0 to 6.0. This finding is consistent with Zp values observed for these systems. In the case of P80, Zp value did not change with pH variation, while for P407, the pH change led to a decrease in Zp value at pH 6.0, resulting in a great capacity of interaction among the micelles.

The micelles formed by P80 were the smallest in size and monodisperse, the mean diameter being around 10 nm, while those formed by P407 presented larger size values and a high polydispersity index, with a mean diameter of around 400 nm. Micellar size of Na-C was larger for ABZ in comparison to RBZ, which might be due to a higher concentration of Na-C in the ABZ micellar system. The parameters could not be determined due to the gelation process in the system prepared with Na-DC and ABZ, while, in the case of Na-DC and RBZ, a great deviation in size values was observed.

DISCUSSION

Fluorescence properties of ABZ and RBZ are favorable to elucidate the process of micellization. Thus, the fluorescence emission process has been used as a tool to determine the capacity of the selected surfactants to solubilize the two anthelmintic drugs.

The Lippert theory predicts a shift in the energy of the optical probe fluorescence emission due to a change in the polarity of the solvent where the fluorophore is located. As a consequence, the maximum emission wavelength (λ_{max}) position of the fluorescence band is a reflex of the environment polarity where the drug is dissolved in the micelle of the surfactants assayed (39,40). Thus, a null or very poor shift in the λ_{max} when ABZ is included in the micelle, as is the case of P407, suggests that the environment has a polar character and the solvent molecules have access to the optical probe. The blue shift from 350 to 345 nm observed when ABZ was included in P80, Na-DC and Na-C, suggests a major non-polar character of the ABZ microenvironment in the micelles of these surfactants. RBZ showed a poor change in the fluorescence band when the molecule was included in the micelle, which could be caused by the presence of a S=O group in its molecule, which is very polar and could deactivate the excited state (34).

The mechanism of micelle formation is usually associated with high cooperativity, multiplicity of organization, and also

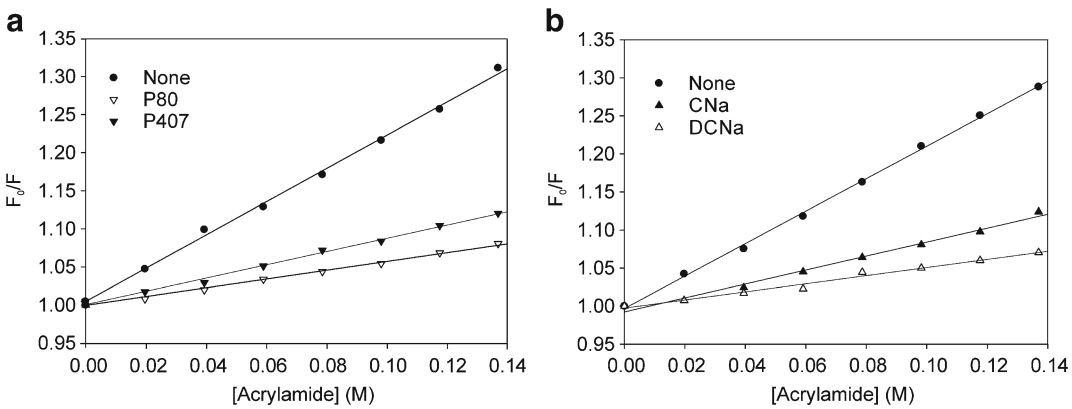

Fig. 4. Stern-Volmer plots for ABZ alone and ABZ incorporated in surfactant micelles. **a** P80 and P407 micelles in citric acid-sodium phosphate dibasic buffer (pH 6.0). **b** Na-C and Na-DC in citric acid-sodium phosphate dibasic buffer (pH 7.0), 20 °C

with the dynamics of micellar environments, such as a non-polar core, a slightly polar palisade layer and a more polar micelle-water interface (30).

Typical ionic and non-ionic surfactants contain a flexible cylindrical body and aggregate in spherical or ellipsoidal micelles with the hydrophobic chains forming a liquid hydrocarbon core (30), allowing the incorporation of the hydrophobic molecules into their interior. Thus, synthetic surfactants have a high capacity to solubilize hydrophobic molecules, as is the case with P407 and P80 assayed in this work.

Bile salts do not behave analogous to conventional surfactants that contain a clear-cut polarity gradient between the hydrophilic and the hydrophobic parts. They show well-defined behavior to self-association and molecular solubilization. The cmc for a given bile salt is largely determined by its hydrophilic-hydrophobic balance. Bile salts are rigid molecules, and when several of them are side by side, the hydrophobic faces are considered to be in contact with each other, while the hydrophilic faces are in contact with the aqueous environment (41). Small *et al.* (42) demonstrated that the micelle formation of bile salts proceeds in two steps: (1) primary micelles of low molecular mass are formed through hydrophobic interactions; (2) secondary micelles are then formed by the aggregation of these primary micelles. As this model involves a polydispersity in the aggregation number, cmc does not appear as a point but as a concentration range (43). This mechanism of micelle formation has two consequences: first, the micelle formation process is highly cooperative, as found in this work; and second, since the hydrophobic molecules are situated among the bile salt molecules forming the micelle, the solubilization capacity of these surfactants is lower than that of the conventional micelle of the synthetic surfactants. Also, this model implies that the inclusion of ABZ and RBZ into these micelles follows a sigmoidal behavior as it was seen from the titration curves. Tenfold higher concentrations of bile salts were required to solubilize a given amount of ABZ or RBZ, in comparison to P80 and P407, which is a clear disadvantage for bile salts as solubilizers. However, bile salts do not have any administration incompatibilities due to their physiological character.

No differences in the solubilization capacity of surfactants P80 and P407 to solubilize ABZ and RBZ were found. Nevertheless, both surfactants were more efficient to protect ABZ than RBZ from the acrylamide attack. In these non-ionic surfactants, solubilization capacity for ABZ was better at pH 4.0 than at pH 6.0.

CONCLUSIONS

In summary, micellar solutions were prepared with two poorly soluble compounds. Fluorescence emission was employed as the main tool to analyze the inclusion of the ABZ and RBZ into the micellar systems. Among the surfactants, P80 and P407 showed higher solubilization capacity than the bile salts assayed, especially for ABZ at pH 4.0. Moreover, P80 micellar system presented the smallest size, monodispersity and good protective efficacy in the quenching experiments. On the other hand, Na-DC had better protective efficacy for ABZ and RBZ, showing the inclusion of the drug into the micelles.

Our results are the first step in the design of novel anti-parasitic solutions so as to improve current pharmaceutical formulations.

ACKNOWLEDGEMENTS

J.P. is grateful to the CONICET (Consejo Nacional de Investigaciones Científicas y Técnicas) for a Doctoral Fellowship. This work was supported by the Universidad Nacional de Rosario, CONICET (Project No. PIP 112-201001-00194) and Agencia Nacional de Promoción Científica y Tecnológica (Project No. PICT 2006-1126). The authors would like to thank Laura Gutierrez and Antonella Giorello from Facultad de Ingeniería Química, Universidad Nacional del Litoral, for Malvern Zetasizer Nano ZS90. We would like to thank the staff from the English Department (Facultad de Ciencias Bioquímicas y Farmacéuticas, Universidad Nacional de Rosario) for the language correction of the manuscript.

REFERENCES

1. Uneke C. Soil transmitted helminth infections and schistosomiasis in school age children in sub-Saharan Africa: efficacy of chemotherapeutic intervention since World Health Assembly Resolution 2001. Tanzan J Health Res. 2010;12(1):86–99.
2. Priotti J, Codina AV, Leonardi D, Vasconi MD, Hinrichsen LI, Lamas MC. Albendazole microcrystal formulations based on chitosan and cellulose derivatives: physicochemical characterization and in vitro parasiticidal activity in Trichinella spiralis adult worms. AAPS PharmSciTech. 2017;18(4):947–56. https://doi.org/10.1208/s12249-016-0659-z.
3. Mascarini-Serra L. Prevention of soil-transmitted helminth infection. J Glob Infect Dis. 2011;3(2):175–82. https://doi.org/10.4103/0974-777X.81696.
4. Castro L, Kviecinski MR, Ourique F, Parisotto EB, Grinevicius V, Correia JFG, *et al.* Albendazole as a promising molecule for tumor control. Redox Biol. 2016;10:90–9. https://doi.org/10.1016/j.redox.2016.09.013.
5. Pranzo MB, Cruickshank D, Coruzzi M, Caira MR, Bettini R. Enantiotropically related albendazole polymorphs. J Pharm Sci. 2010;99(9):3731–42. https://doi.org/10.1002/jps.22072.
6. Wu Z, Razzak M, Tucker IG, Medlicott NJ. Physicochemical characterization of ricobendazole: I. Solubility, lipophilicity, and ionization characteristics. J Pharm Sci. 94(5):983–93.
7. Yadav D, Kumar N. Nanonization of curcumin by antisolvent precipitation: process development, characterization, freeze drying and stability performance. Int J Pharm. 2014;477(1–2):564–77. https://doi.org/10.1016/j.ijpharm.2014.10.070.
8. García A, Leonardi D, Salazar MO, Lamas MC. Modified β-cyclodextrin inclusion complex to improve the physicochemical properties of albendazole. Complete in vitro evaluation and characterization. PLoS One. 2014;9(2):e88234. https://doi.org/10.1371/journal.pone.0088234.
9. Castro SG, Bruni SS, Lanusse CE, Allemandi DA, Palma SD. Improved albendazole dissolution rate in pluronic 188 solid dispersions. AAPS PharmSciTech. 2010;11(4):1518–25. https://doi.org/10.1208/s12249-010-9517-6.
10. Wu Z, Razzak M, Tucker IG, Medlicott NJ. Physicochemical characterization of ricobendazole: I. Solubility, lipophilicity, and ionization characteristics. J Pharm Sci. 2005;94(5):983–93. https://doi.org/10.1002/jps.20282.
11. Wu Z, Tucker IG, Razzak M, Medlicott NJ. Stability of ricobendazole in aqueous solutions. J Pharm Biomed Anal. 2009;49(5):1282–6. https://doi.org/10.1016/j.jpba.2009.02.032.
12. Fernández L, Sigal E, Otero L, Silber J, Santo M. Solubility improvement of an anthelmintic benzimidazole carbamate by

association with dendrimers. Braz J Chem Eng. 2011;28(4):679–89. https://doi.org/10.1590/S0104-66322011000400013.
13. Motlagh NSH, Parvin P, Ghasemi F, Atyabi F. Fluorescence properties of several chemotherapy drugs: doxorubicin, paclitaxel and bleomycin. Biomed Opt Express. 2016;7(6):2400–6. https://doi.org/10.1364/BOE.7.002400.
14. Salahuddin, Shaharyar M, Mazumder A. Benzimidazoles: a biologically active compounds. Arab J Chem. 2017;10(1):S157–S73. https://doi.org/10.1016/j.arabjc.2012.07.017.
15. Shvadchak VV, Kucherak O, Afitska K, Dziuba D, Yushchenko DA. Environmentally sensitive probes for monitoring protein-membrane interactions at nanomolar concentrations. Biochim Biophys Acta. 2017;1859(5):852–9. https://doi.org/10.1016/j.bbamem.2017.01.021.
16. Calafato NR, Picó G. Griseofulvin and ketoconazole solubilization by bile salts studied using fluorescence spectroscopy. Colloids Surf B Biointerfaces. 2006;47(2):198–204. https://doi.org/10.1016/j.colsurfb.2005.01.007.
17. Piñeiro L, Novo M, Al-Soufi W. Fluorescence emission of pyrene in surfactant solutions. Adv Colloid Interface Sci. 2015;215(Supplement C):1–12.
18. Stępnik KE, Malinowska I. Determination of binding properties of ampicillin in drug-human serum albumin standard solution using N-vinylpyrrolidone copolymer combined with the micellar systems. Talanta. 2017;162:241–8. https://doi.org/10.1016/j.talanta.2016.09.054.
19. Ashok B, Arleth L, Hjelm RP, Rubinstein I, Önyüksel H. In vitro characterization of PEGylated phospholipid micelles for improved drug solubilization: effects of PEG chain length and PC incorporation. J Pharm Sci. 2004;93(10):2476–87. https://doi.org/10.1002/jps.20150.
20. Calabrese I, Gelardi G, Merli M, Liveri MLT, Sciascia L. Clay-biosurfactant materials as functional drug delivery systems: slowing down effect in the in vitro release of cinnamic acid. Appl Clay Sci. 2017;135:567–74. https://doi.org/10.1016/j.clay.2016.10.039.
21. Croy SR, Kwon GS. Polysorbate 80 and cremophor EL micelles deaggregate and solubilize nystatin at the core–corona interface. J Pharm Sci. 2005;94(11):2345–54. https://doi.org/10.1002/jps.20301.
22. Cheng M, Zeng G, Huang D, Yang C, Lai C, Zhang C, *et al*. Advantages and challenges of Tween 80 surfactant-enhanced technologies for the remediation of soils contaminated with hydrophobic organic compounds. Chem Eng J. 2017;314:98–113. https://doi.org/10.1016/j.cej.2016.12.135.
23. Ćirin D, Krstonošić V, Poša M. Properties of poloxamer 407 and polysorbate mixed micelles: influence of polysorbate hydrophobic chain. J Ind Eng Chem. 2017;47:194–201. https://doi.org/10.1016/j.jiec.2016.11.032.
24. Adams ML, Lavasanifar A, Kwon GS. Amphiphilic block copolymers for drug delivery. J Pharm Sci. 2003;92(7):1343–55. https://doi.org/10.1002/jps.10397.
25. Pitto-Barry A, Barry NPE. Pluronic[registered sign] block-copolymers in medicine: from chemical and biological versatility to rationalisation and clinical advances. Polym Chem. 2014;5(10):3291–7. https://doi.org/10.1039/C4PY00039K.
26. Chavda S, Danino D, Aswal VK, Singh K, Marangoni DG, Bahadur P. Microstructure and transitions in mixed micelles of cetyltrimethylammonium tosylate and bile salts. Colloids Surf A Physicochem Eng Asp. 2017;513:223–33. https://doi.org/10.1016/j.colsurfa.2016.10.047.
27. Holm R, Müllertz A, Mu H. Bile salts and their importance for drug absorption. Int J Pharm. 2013;453(1):44–55. https://doi.org/10.1016/j.ijpharm.2013.04.003.
28. Hidalgo-Rodríguez M, Fuguet E, Ràfols C, Rosés M. Solute–solvent interactions in micellar electrokinetic chromatography: VII. Characterization of sodium cholate–sodium deoxycholate mixed-micellar systems. J Chromatogr A. 2010;1217(10):1701–8. https://doi.org/10.1016/j.chroma.2010.01.001.
29. Selvam S, Andrews ME, Mishra AK. A photophysical study on the role of bile salt hydrophobicity in solubilizing amphotericin B aggregates. J Pharm Sci. 2009;98(11):4153–60. https://doi.org/10.1002/jps.21718.
30. Martin AN, Bustamante P. Physical pharmacy: physical chemical principles in the pharmaceutical sciences. 4th ed. Philadelphia: Lea & Febiger; 1993.
31. Sepúlveda L, Pérez-Cotapos J. Interactions between alkyl xanthates and cationic micelles. J Colloid Interface Sci. 1986;109(1):21–30. https://doi.org/10.1016/0021-9797(86)90277-8.
32. Enache M, Volanschi E. Spectral studies on the molecular interaction of anticancer drug mitoxantrone with CTAB micelles. J Pharm Sci. 2011;100(2):558–65. https://doi.org/10.1002/jps.22289.
33. Jindal N, Mehta SK. Nevirapine loaded Poloxamer 407/Pluronic P123 mixed micelles: optimization of formulation and in vitro evaluation. Colloids Surf B Biointerfaces. 2015;129:100–6. https://doi.org/10.1016/j.colsurfb.2015.03.030.
34. Lackowicz JR. Principles of fluorescence spectroscopy. 3rd ed. New York: Plenum Press; 1983. https://doi.org/10.1007/978-1-4615-7658-7.
35. Suksiriworapong J, Rungvimolsin T, Ag-omol A, Junyaprasert VB, Chantasart D. Development and characterization of lyophilized diazepam-loaded polymeric micelles. AAPS PharmSciTech. 2014;15(1):52–64. https://doi.org/10.1208/s12249-013-0032-4.
36. Balakrishnan A, Rege BD, Amidon GL, Polli JE. Surfactant-mediated dissolution: contributions of solubility enhancement and relatively low micelle diffusivity. J Pharm Sci. 2004;93(8):2064–75. https://doi.org/10.1002/jps.20118.
37. Markina A, Ivanov V, Komarov P, Khokhlov A, Tung SH. Self-assembly of micelles in organic solutions of lecithin and bile salt: mesoscale computer simulation. Chem Phys Lett. 2016;664:16–22. https://doi.org/10.1016/j.cplett.2016.09.078.
38. Kaya A, Yukselen Y. Zeta potential of soils with surfactants and its relevance to electrokinetic remediation. J Hazard Mater. 2005;120(1–3):119–26. https://doi.org/10.1016/j.jhazmat.2004.12.023.
39. Mallick A, Purkayastha P, Chattopadhyay N. Photoprocesses of excited molecules in confined liquid environments: an overview. J Photochem Photobiol C Photochem Rev. 2007;8(3):109–27. https://doi.org/10.1016/j.jphotochemrev.2007.06.001.
40. Nayak MK, Dogra SK. Solvatochromism and prototropism in methyl 6-aminonicotinate: failure to observe amine-imine phototautomerism in solvents. J Mol Struct. 2004;702(1–3):85–94. https://doi.org/10.1016/j.molstruc.2004.06.014.
41. Subuddhi U, Mishra AK. Micellization of bile salts in aqueous medium: a fluorescence study. Colloids Surf B Biointerfaces. 2007;57(1):102–7. https://doi.org/10.1016/j.colsurfb.2007.01.009.
42. Small DM, Penkett SA, Chapman D. Studies on simple and mixed bile salt micelles by nuclear magnetic resonance spectroscopy. Biochim Biophys Acta. 1969;176(1):178–89. https://doi.org/10.1016/0005-2760(69)90086-1.
43. Raupp G, Felippe AC, Frizon TEA, Silva L, Paula MMS, Dal-Bó AG. Determination of the stabilization time of the solution-air interface for aggregates formed by NaC in mixtures with SDS and PEO, investigated by dynamic surface tension measurements. Soft. 2014;3:1–10.